

A novel maskless approach towards aligned, density modulated and multi-junction ZnO nanowires for enhanced surface area and light trapping solar cells

This article has been downloaded from IOPscience. Please scroll down to see the full text article.

2010 Nanotechnology 21 315602

(<http://iopscience.iop.org/0957-4484/21/31/315602>)

View [the table of contents for this issue](#), or go to the [journal homepage](#) for more

Download details:

IP Address: 137.132.123.69

The article was downloaded on 20/07/2010 at 01:39

Please note that [terms and conditions apply](#).

A novel maskless approach towards aligned, density modulated and multi-junction ZnO nanowires for enhanced surface area and light trapping solar cells

M Kevin¹, Y H Fou¹, A S W Wong² and G W Ho^{1,3}

¹ Department of Electrical and Computer Engineering, National University of Singapore, 4 Engineering Drive 3, Singapore 117576, Singapore

² Institute of Materials Research and Engineering, A*STAR (Agency for Science Technology and Research), 3 Research Link, Singapore 117602, Singapore

E-mail: elehgw@nus.edu.sg

Received 17 March 2010, in final form 4 June 2010

Published 15 July 2010

Online at stacks.iop.org/Nano/21/315602

Abstract

A maskless method of employing polymer growth inhibitor layers is used to modulate the conflicting parameters of density and alignment of multi-junction nanowires via large-scale low temperature chemical route. This low temperature chemical route is shown to synthesize multi-junction nanostructures without compromising the crystal quality at the interfaces. The final morphology of optimized multi-junction nanowire arrays can be demonstrated on various substrates due to substrate independence and low temperature processing. Here, we also fabricated devices based on density modulated multi-junction nanowires tuned to infiltrate nanoparticles. The fabrication of hierarchically structured nanowire/nanoparticles composites presents an advantageous structure, one that allows nanoparticles to provide large surface areas for dye adsorption, whilst the nanowires can enhance the light harvesting, electron transport rate, and also the mechanical properties of the films. This work can be of great scientific and commercial interest since the technique employed is of low temperature (<90 °C) and economical for large-scale solution processing, much valued in today's flexible display and photovoltaic industries.

(Some figures in this article are in colour only in the electronic version)

1. Introduction

For fabrication of nanodevices, the density and alignment modulation of nanowires on various substrates is very important since it is directly related to how the nanowires interact with each other optically, electronically, chemically or mechanically. For instance, in the case of catalytic nanodevices, high density interconnected nanowires are favorable whereas for field emission devices, sparsely packed aligned nanowires are preferred for high field enhancement

exhibition. In addition, fabrication of nanostructures with greater complexity such as axially modulated junctions of the same or different compositions (longitudinal heterojunctions) will introduce many new opportunities for enhancing device functionality. Such heterostructures with tailored segments of different functionalities along the same nanowire are expected to exhibit unique optical and electrical properties which will become increasingly important to the development of advanced nanoelectronic and nanophotonic systems [1–6]. For example, a single semiconductor nanowire containing a p-type segment and an n-type segment can be used as an intrawire p–n junction,

³ Author to whom any correspondence should be addressed.

which has found applications in field-effect transistors (FETs) and single-nanowire light-emitting diodes (LEDs) [1].

So far, the most common technique used to control the density and alignment of nanowires is top down lithography and etching or adjusting the thickness of the metal catalyst layer [7–9]. Although they can offer precise control, stringent requirements such as high reaction temperature, single crystalline substrate, complex processing and expensive equipment are needed. As for the case of the low temperature chemical route, the density control of nanowires has always been achieved via tuning of seed layer thickness [10, 11]. However, the change in the density is limited and usually at the cost of the nanowires' alignment. In regard to the multi-junction synthesis, one-dimensional (1D) doped nanowires have mainly been synthesized by vapor-phase techniques which rely mainly on the vapor–liquid–solid (VLS) mechanism in which the alternate growth of different segments can be achieved by modulation of the vapor-phase reactants during growth of the wires. Similarly, stringent requirements such as high reaction temperature, complex processing and equipment are needed.

Our idea is to simply exploit a polymer inhibitor layer to control both conflicting parameters of density and alignment of multi-junction nanowires via the low temperature solution phase. The creation of multi-junctions along the axial direction of nanowires was demonstrated with few cycles of secondary growth without compromising the crystal quality at the interfaces. This maskless method address the issue of growing nanowires of modulated density with good alignment without undergoing any lithographic or templating top down techniques. Furthermore, device demonstrations on these multi-junction nanowires were presented. We demonstrated that the density modulated multi-junction nanowires can be tuned to infiltrate nanoparticles, creating a hybrid hierarchically structured nanowire/nanoparticles solar cell. Semiconducting nanowire arrays are known for low reflective losses and efficient electron transport. The motivation for fabrication of such hierarchically structured nanowire/nanoparticles composites is due to its advantageous structure, one that allows nanoparticles to provide large surface areas for dye adsorption, whilst the nanowires can enhance the light harvesting, electron transport rate, and also the mechanical properties of the films. There has been limited investigation on such structural systems due to the inability of the nanoparticles to infiltrate into densely packed arrays of nanowires. This work can be of great scientific and commercial interest since the technique employed is of low temperature (<90 °C) and economical for large-scale solution processing, much valued in today's flexible display and photovoltaic industries.

2. Experimental section

Si(100), plastic and FTO glass substrates were cleaned using isopropyl alcohol (IPA) and absolute ethanol in an ultrasonic bath for 10 min each. The substrates were then irradiated under ultraviolet light using a mercury vapor lamp (Novascan)

for 10 min to remove residual organic contaminants. 10–40 mg of zinc acetate (ZnAc) and 0.3 g of polyvinylpyrrolidone (PVP) were dissolved in 5.0 ml of absolute ethanol. The seed solution was spin coated onto the pre-washed FTO substrates at 3000 rpm for 1 min. The PVP forms a polymer matrix in which zinc acetate can be well dispersed on the substrate. PVP also aids in improving the wettability of the seed solution on the substrate. Subsequent heat treatment at 550 °C for 2 h removes the PVP and at the same time thermally decomposes zinc acetate to form ZnO nanocrystals. The well-dispersed ZnO nanocrystals act as nucleation sites for the growth of ZnO nanowires. Growth precursor was prepared as follows: an aqueous 25 mM zinc nitrate hexahydrate and hexamethylenetetramine (HMT) solution was prepared, into which 0.1 g of polyethyleneimine (PEI) was added to 50 ml of aqueous precursor. Seeded substrates were suspended upside down in the growth precursor and left to stand for 2 h at 90 °C. Subsequent, secondary growth was performed using 3% polymethyl methacrylate (PMMA) dissolved in 1:3 methyl isobutyl ketone (MIBK) and isopropyl alcohol (IPA) solvent which was spin coated directly onto the primary nanowires and the substrate was then baked at 150 °C for 3 min and before they were regrown in a fresh batch of growth precursor. The soft baking step at 150 °C aims to improve polymer inhibitor adhesion to the primary nanowires. In addition, soft baking can prevent the heat treated polymer inhibitor layer from dissolving in the subsequent secondary growth process. ZnO nanoparticles were spin coated onto into the multi-junction nanowire array. The FTO substrate was immersed for 1 h in *cis*-bis(isothiocyanato) bis(2,20-bipyridyl-4,40-dicarboxylato)-ruthenium(II)bis-tetrabutylammonium (0.3 mM, N719 Solaronix) with absolute ethanol as the solvent. The counter electrode consisted of a Pt/FTO substrate deposited using RF magnetron sputtering. The electrolyte solution used consisted of 0.1 M lithium iodide, 0.03 M iodine, 0.5 M 4-*tert*-butylpyridine and 0.6 M 1-propyl-2,3-dimethyl imidazolium iodide with acetonitrile as the solvent.

Scanning electron microscopy (SEM) observations were carried out on a FESEM JSM-6700F operating at 10 kV. Transmission electron microscopy (TEM) characterizations were conducted using a JEOL-2100 TEM with an accelerating voltage of 200 kV. X-ray diffraction (XRD) experiments were performed on a Bruker GADDS XRD using monochromatized Cu K α ($\lambda = 0.154$ nm) radiation under 40 kV and 40 mA. The absorption spectra were obtained using UV–vis spectrophotometer (UV-1800 Shimadzu). *I*–*V* characterizations were carried out using a Keithley 4200 SCS SourceMeter. The photocurrent voltage of these samples was measured with a solar simulator (model 69907 Newport) system under 1 sun at an air mass (AM) 1.5 global filter (1000 W m⁻²) equipped with 150 W ozone free xenon lamp.

3. Results and discussion

Since the growth of ZnO nanowires are initiated by the introduction of the seed layer which acts as the nucleation sites, the most straightforward method to control the nanowires' density is by modifying the thickness or concentration of the

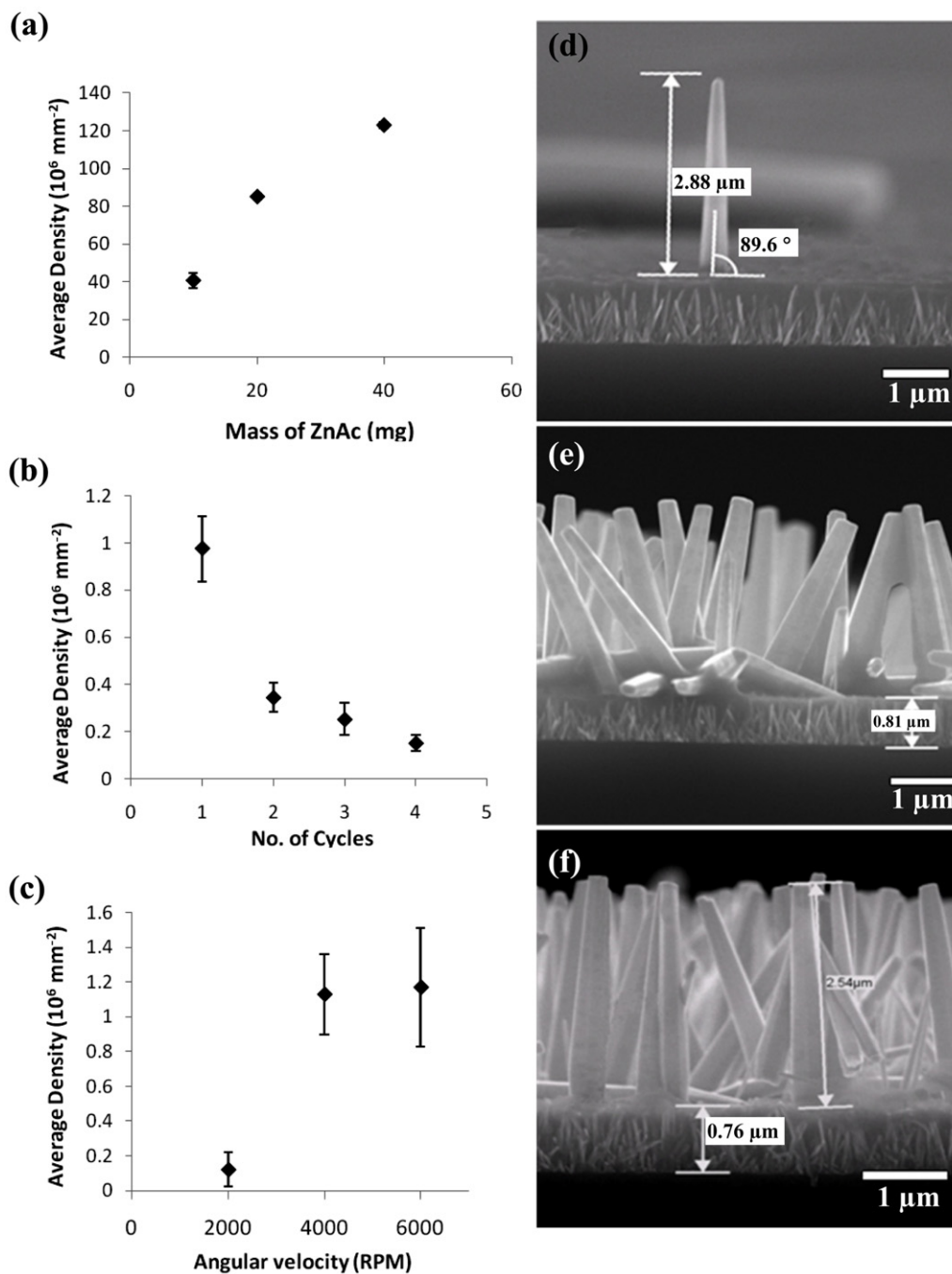


Figure 1. Graph of nanowire density against different (a) mass of ZnAc, (b) number of cycles and (c) different angular velocities. SEM images multi-junction nanowires grown by different polymer thickness (d) $0.93 \mu\text{m}$ at 2000 rpm (e) $0.81 \mu\text{m}$ at 4000 rpm and (f) $0.75 \mu\text{m}$ at 6000 rpm.

seed layer. Figure 1(a) summarizes the nanowires density as a function of different seed concentration. The densities of nanowires are 40.7 , 87.5 and 123.6×10^6 nanowires mm^{-2} with 10 , 20 and 40 mg ZnAc respectively. The concentration of the seed layer controls not only the nanowire density but also has a strong impact on the orientation of the nanowire arrays. It can be observed that the density of nanowires as well as the alignment of the nanowires decreases with the concentration of the seed layer. This phenomenon can be explained by the fact that a sparsely distributed seed layer causes low density growth

of nanowires which in turn weaken the effect of interaction (steric hindrance) among the nanowires. Hence the nanowires grow freely (unoriented) without obstacles thus rendering a poorer alignment.

In view of the problems encountered in achieving low density and at the same time having well-aligned nanowires, we have utilized polymer inhibitor coating to resolve these conflicting factors. Multi-layer polymer coating (with fixed angular velocity/thickness) and few cycles of secondary growth were carried out. The schematic diagram of figure 2 depicts the

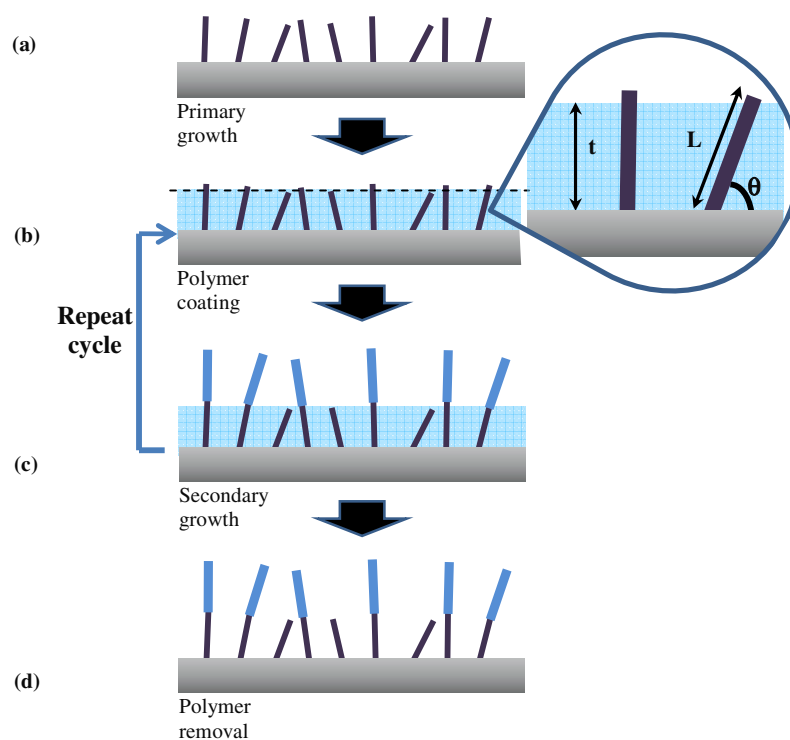


Figure 2. Process flow of the nanowires with multi-layer polymer coatings. (a) Primary growth (b) polymer coating (c) secondary growth and (d) removal of polymer.

process flow that was carried out. An initial array of nanowires is first grown (primary growth) as shown in figure 2(a). A layer of polymer (3% PMMA) is then spin coated directly onto the primary nanowires (figure 2(b)). The substrate is then baked at 150 °C for 3 min and was then grown again in a fresh batch of growth precursor (secondary growth) as shown in figure 2(c). The cycle was repeated several times to modulate the density and alignment of the nanowires. Eventually, the polymer coating was removed using acetone (figure 2(d)). In figure 2(b) (high magnification), a polymer inhibitor coating of thickness t is used to select nanowires which are grown nearly normal to the surface ($\theta \sim 90^\circ$). Therefore, only fairly aligned nanowires are sufficiently long to protrude from within the polymer matrix to participate in the secondary growth. These participating nanowires satisfy the condition of having length of $L \sin \theta > t$. In general, it is observed that the nanowires grow at approximately the same rate, meaning that the fairly aligned nanowires will have a higher chance to participate in the secondary growth. Figure 1(b) shows the plot of the density of nanowires versus the number of polymer coating with fixed angular velocity of 4000 rpm. The density of nanowire decreased with multi-layer polymer coating as such the densities of nanowires for primary growth and secondary growth with single, bi- and tri-layer of polymer coating are 0.97 , 0.35 , 0.25 and 0.15×10^6 nanowires mm^{-2} . This is expected since only nanowires that are sufficiently long and/or aligned protruded out of the polymer matrix to take part in the secondary growth.

Another effective way to modulate nanowire density is to vary the thickness of the polymer layer instead of performing multi-layer coating which is quite laborious and

prone to nanowire breakages due to multiple processing steps. However, it is noted that to create complex structured nanowires, the multi-layer coating method will be required to produce multi-junction nanowires. Figure 1(c) summarizes the nanowires density as a function of four different angular velocities. Figures 1(d)–(f) shows the SEM images of the polymer coating with various angular velocities. Figure 1(d) shows the secondary grown nanowire is almost vertically aligned ($\sim 89.6^\circ$) even when the density of nanowires is extremely low. The densities of nanowires are 0.15 , 1.14 and 1.18×10^6 nanowires mm^{-2} with polymer thickness of 0.93 , 0.81 and $0.71 \mu\text{m}$ at 2000, 4000 and 6000 rpm respectively. Thus, the density of the nanowires increases with decreasing polymer thickness since at higher angular velocities, the polymer coating can be made thinner, allowing more nanowires to satisfy the condition $L \sin \theta > t$ and vice versa.

In addition to the density modulation, we have also attempted to do other structural control. It is observed that the secondary grown nanowires generally have ‘heavy-top’, or larger diameter (diameter range 200–500 nm) than the primary nanowires as shown in figure 3(a) (before polymer removal). These ‘heavy-top’ nanowires are susceptible to structural collapse upon removal of polymer coating (as indicated by an arrow in figure 3(b)). High magnification image (figure 3(c)) of the secondary grown nanowire (after the removal of polymer coating) shows diameter of ~ 200 nm as compared to the primary grown nanowire of ~ 40 nm. The secondary grown nanowires are ~ 5 times larger in diameter than the primary nanowires. The ‘heavy-top’ nanowires can be tuned by reducing the subsequent growth precursor concentration. Thus taking into account the lower nucleation

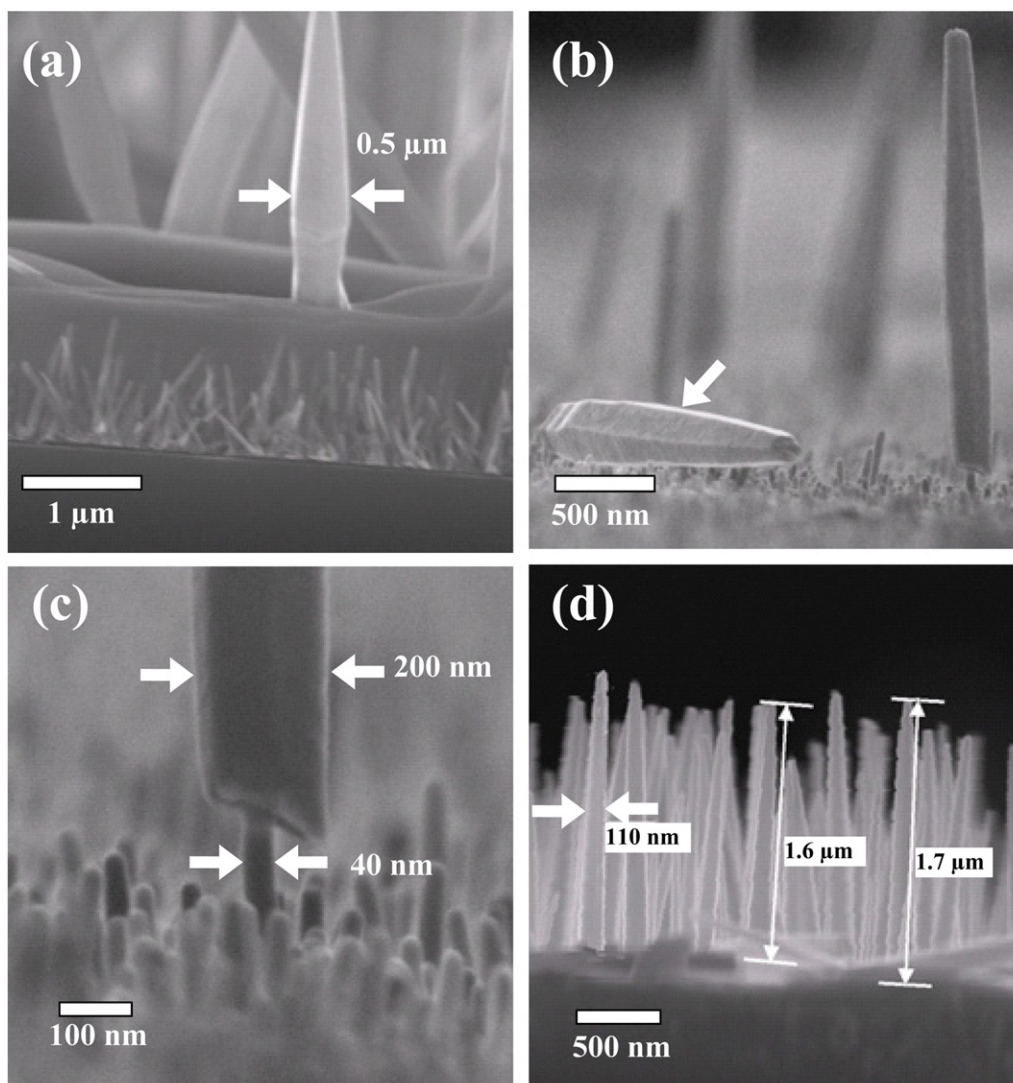


Figure 3. (a) ‘Heavy-top’ secondary nanowires (before polymer removal). (b) ‘heavy-top’ nanowires are susceptible to structural collapse upon the removal of polymer coating (as indicated by an arrow). (c) High magnification image of a multi-junction nanowire. (d) Secondary grown nanowires of thinner diameter with reduced precursor concentration.

sites for the secondary growth, the precursor concentration was decreased. Figure 3(d) shows the secondary grown nanowires of diameter ~ 110 nm and primary nanowire of ~ 50 nm after reducing the precursor concentration by twice the amount. Further control of precursor concentration has allowed us to reproducibly obtain secondary grown nanowires of ~ 1.5 – 2 times the diameter of the primary nanowires. It is also noted that the nanowires grown with reduced precursor concentration (figure 3(d)) still retain a good alignment of 80° – 90° . Another structural tuning that we have carried out is to control the underlying density of the primary nanowire array. The control of the density of the primary nanowire is important since it will determine the effectiveness of the polymer coating. A high density primary nanowire array does not allow polymer penetration, causing much of the polymer to reside above the nanowires, thus blocking most of the nanowires nucleation sites. Hence, secondary growth of nanowires becomes extremely sparse. Figure 4(a) shows the secondary grown nanowires (after removal of polymer coating)

with high seed concentration of 40 mg which yields high density of primary nanowire array, thus rendering the sparse distribution of secondary grown nanowires. On the other hand, in the case of a low density primary nanowire array, there are statistically too few nanowires that were well oriented and this also causes the secondary growth to be sparsely distributed as well. After much optimization, the primary seed layer of 20 mg gives the optimum nanowire dimensions and orientation for the secondary layer as shown in figure 4(b) on Si and figures 4(c) and (d) on FTO substrates. The type of substrate used for the growth of the nanowires (both primary and secondary growth) has little effect and the results can also be reproduced on plastic and glass substrate. The substrate independence and low temperature growth can be of great commercial interest.

Structural characterizations are performed on the ZnO nanowire with secondary growth using TEM. A representative low magnification TEM image of an optimized multi-junction nanowire with primary nanowire diameter of ~ 50 nm and secondary nanowire diameter of ~ 80 nm is shown in

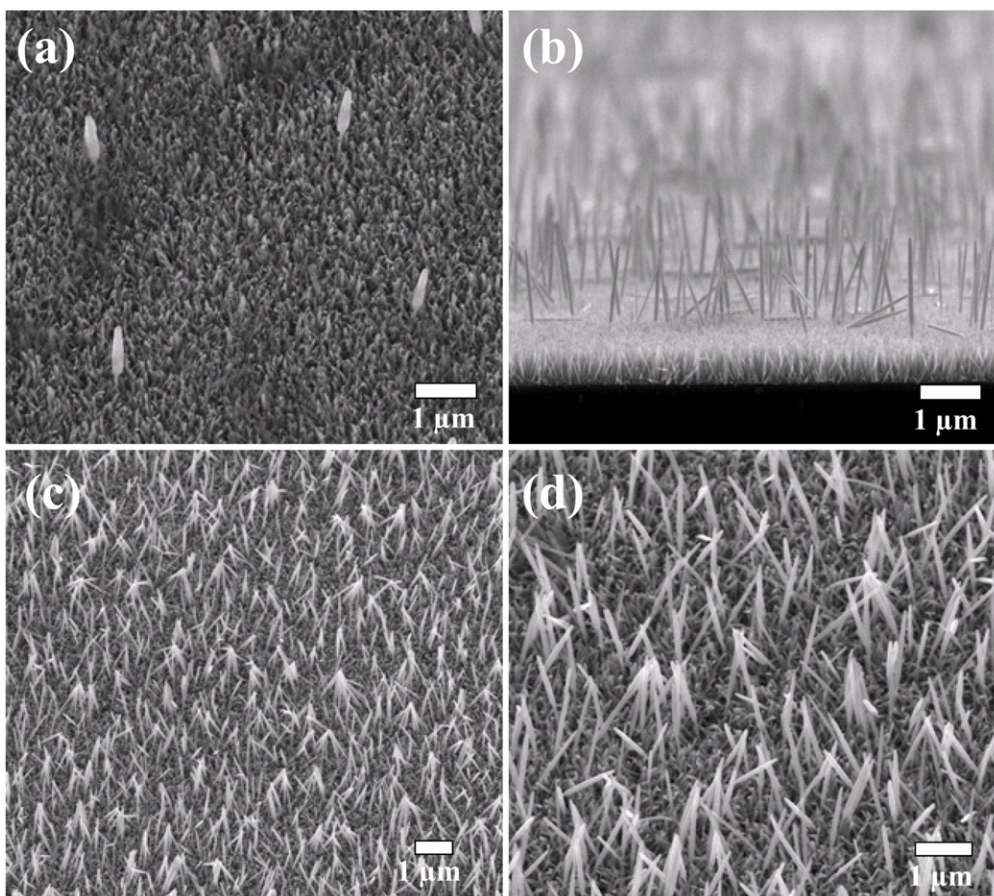


Figure 4. (a) Sparsely grown secondary nanowires with high density primary nanowires. Multi-junction nanowires on (b) Si and (c)–(d) FTO substrates at different magnifications.

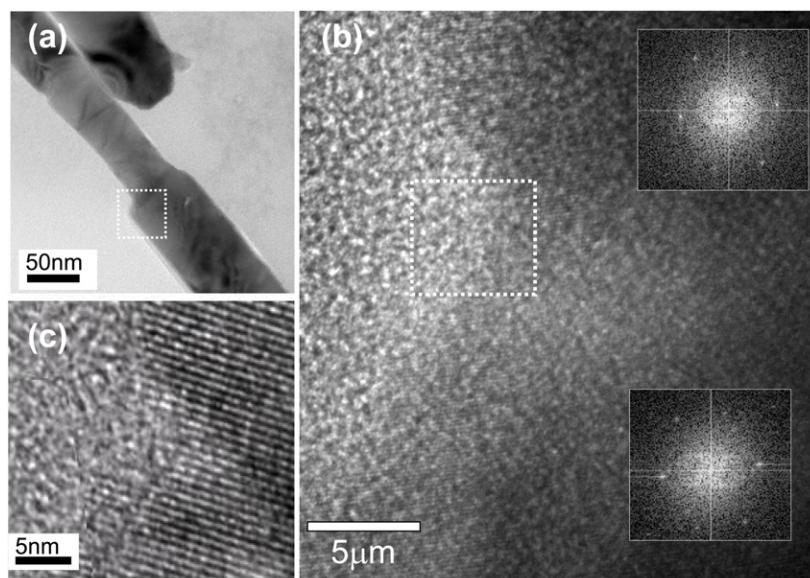


Figure 5. TEM characterizations of (a) low magnification and (b)–(c) high resolution images at the junction of two segments of a nanowire. Inset of (b) shows the FFT obtained at the interface region.

figure 5(a). At higher resolution of the marked area of the multi-junction nanowire of figure 5(a), Fourier transform of the two segment nanowires (insets) shows the same interplanar distance near the junction area (figure 5(b)). In addition, high

resolution image (figure 5(c)) shows clear lattice fringes for both nanowire segments at the junction interface which suggest the epitaxial relationship of the two nanowire segments. The low temperature chemical route has synthesized multi-

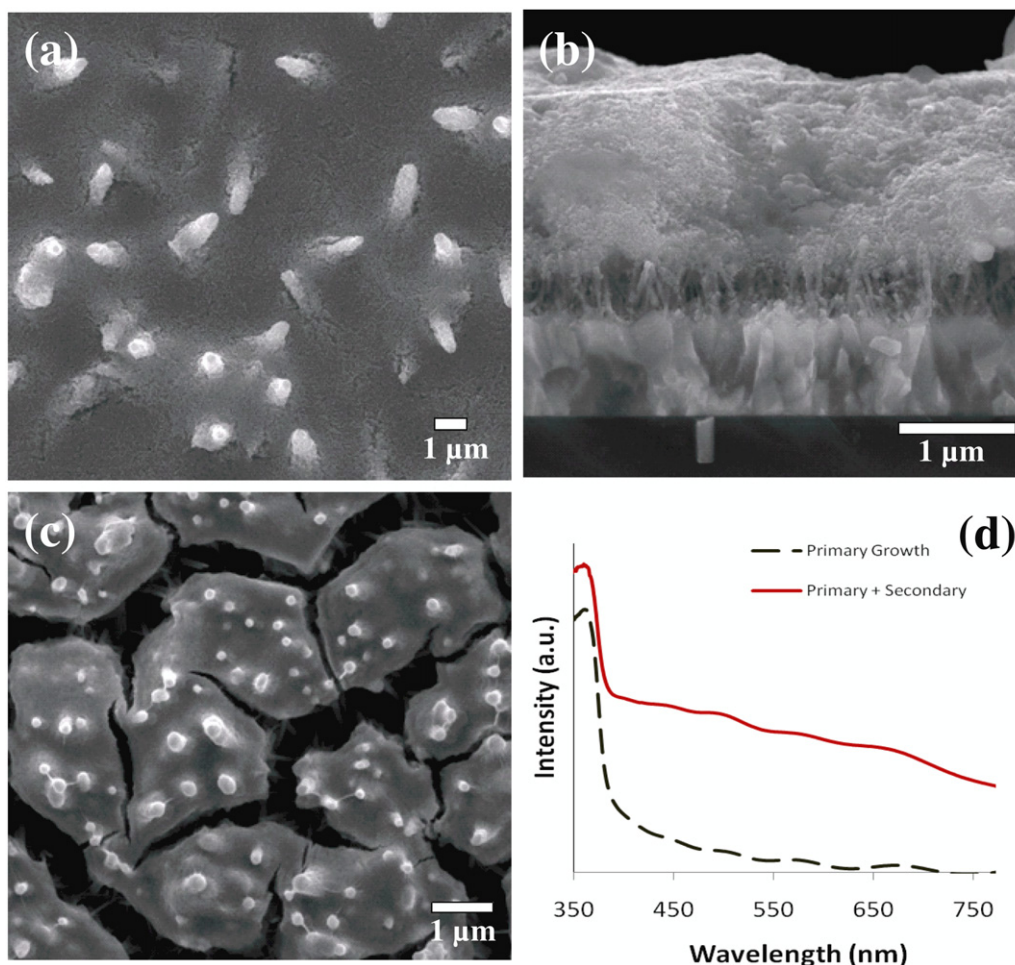


Figure 6. SEM images (a)–(b) top and cross-section of the multi-junction nanowires with infiltrated nanoparticles and (c) densely packed primary nanowires with non-penetrated nanoparticles and cracked film morphology. (d) Optical absorbance spectra of primary and multi-junction nanowires.

junction nanowire without compromising the crystal quality at the interfaces. We believe that the epitaxial interface is formed between the two segments of nanowires due to the effectiveness of atomic interdiffusion restructuring across the junctions in the solution phase [12]. The lattice fringes have interplanar spacing of ~ 0.52 nm which confirms that the ZnO nanowires are single crystalline with a preferential growth in the [0001] direction (figure 5(c)), supporting the XRD results (not shown here) [13].

Device demonstrations based on solar cells are also carried out. The motivation comes from the fact that the semiconducting nanowire arrays are known for low reflective losses and efficient electron transport. Three solar cells consist of ZnO nanoparticles, nanowires and the hybrid nanowire and nanoparticles were fabricated. The density modulated multi-junction nanowires were able to infiltrate nanoparticles to create a hybrid hierarchically structured nanowire/nanoparticles solar cell (figures 6(a) and (b)). The densely packed primary layer nanowires served as a diffusion barrier layer while the secondary nanowires serve as the scaffold for the infiltration of the ZnO nanoparticles. The hierarchically structured

nanowire/nanoparticles composites represent an advantageous structure, one that allows nanoparticles to provide large surface areas for dye adsorption, whilst the nanowires can enhance the light harvesting, electron transport rate, and also the mechanical properties of the films. There has been limited investigation on such structural system due to the inability of the nanoparticles to infiltrate into the densely packed primary nanowires as shown in figure 6(c). Optical absorption measurements were performed over the spectral range from 350 to 800 nm (figure 6(d)). There is a large intensity increase in the absorbed light with the hierarchically structured nanowire/nanoparticle film, suggesting strong light trapping within the hybrid film matrix. From the absorption spectra, it is apparent that there is a great improvement in both ultraviolet and visible light range due to the contribution of periodically arranged nanowires and the incorporated nanoparticle hybrid film. Figure 7 (insets) shows the I – V characteristics and summary of the photovoltaic properties of various solar cells. The J_{sc} and the light conversion efficiency of the hierarchical structure were higher than that of the ZnO nanoparticles or nanowires solar cells. One reason for the increase in J_{sc} is the enhanced absorption behavior associated with

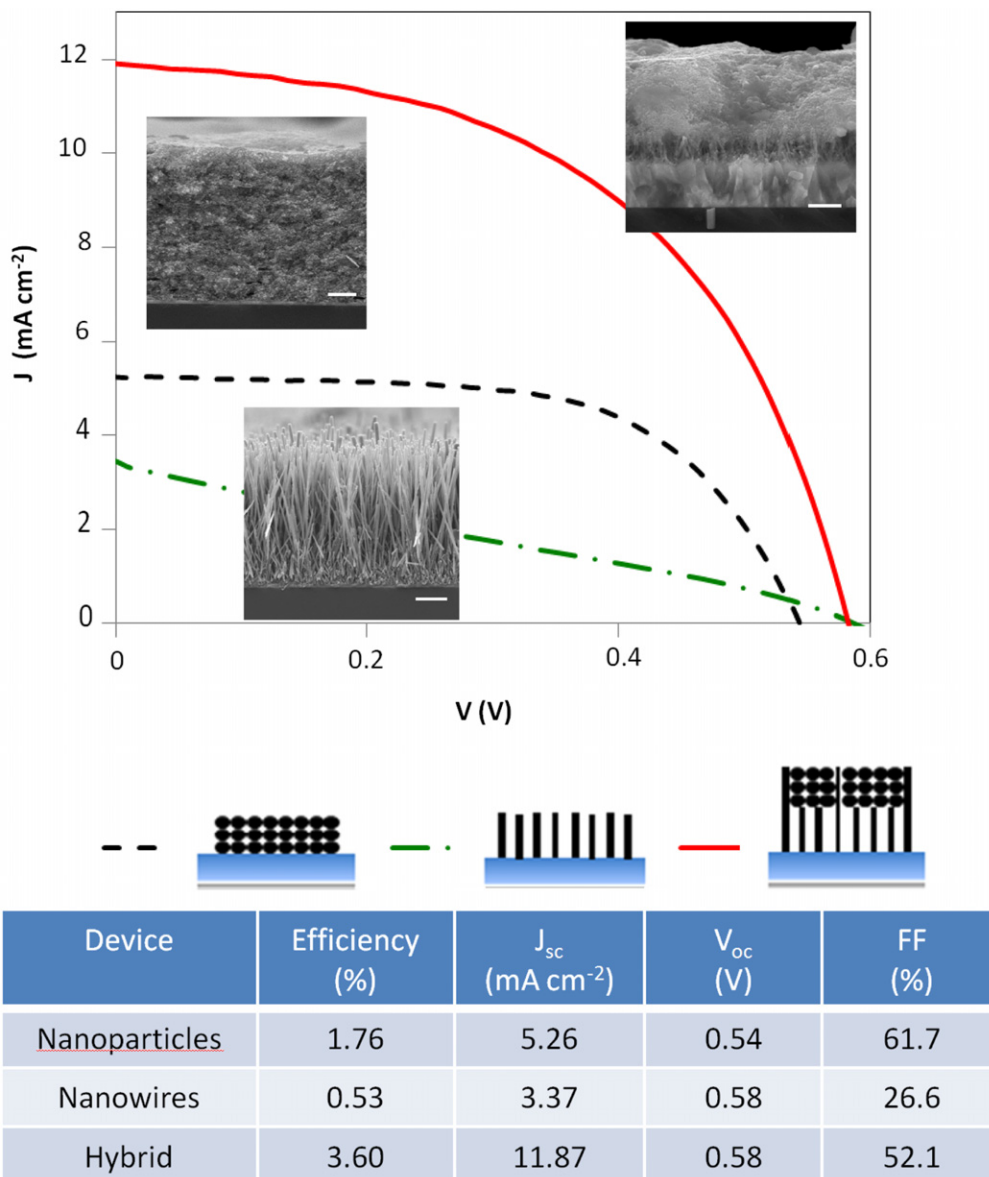


Figure 7. I - V characteristics and summary of the photovoltaic properties of various ZnO structural compositions. Insets show the SEM images of the various ZnO nanostructures solar cells. Scale bar: $1 \mu\text{m}$.

the presence of large surface area nanoparticles and the light trapping capability of nanowires, resulting in higher photon absorption (complements the absorption results). The hierarchical structured solar cell is promising since one-dimensional nanostructures have proven to facilitate electron transport unlike the nanoparticles; electron transport is a slow trap-limited diffusion process. It has been reported that the electron diffusion coefficient of ZnO nanowires can be several hundred times larger than the coefficient for ZnO or TiO_2 nanoparticle film [14]. The rapid electron transport in the 1D inorganic nanostructure based solar cells is important to ensure efficient collection by the conducting substrate before recombination processes occur. From the above discussion, we believe that there is still plenty of room for optimizing the hybrid nanowires/nanoparticles towards highly efficient solar cells.

4. Conclusion

The creation of multi-junctions along the axial direction of nanowires was demonstrated with few cycles of secondary growth without compromising the interface crystal quality and transport characteristics. Vertically aligned and density modulated nanowires can be mass produced and deposited using low cost procedures on various inexpensive and flexible substrates due to substrate independence and low temperature processing. This work complements all the exciting efforts focused on improving and realizing the electrical and structural properties of electronics devices and solar cells through facile and low temperature techniques. In addition to the exciting possibilities for solar technology, this work can be generalized for photodetectors, imagers, sensors, and solid-state lighting applications.

Acknowledgments

This work is supported by the National University of Singapore (NUS) grant and Applied Materials.

References

- [1] Gudiksen M S, Lauhon L J, Wang J, Smith D C and Lieber C M 2002 *Nature* **415** 617
- [2] Wu Y, Fan R and Yang P 2002 *Nano Lett.* **2** 83
- [3] Björk M T, Ohlsson B J, Sass T, Persson A I, Thelander C, Magnusson M H, Deppert K, Wallenberg L R and Samuelson L 2002 *Nano Lett.* **2** 87
- [4] Wu Y, Xiang J, Yang C, Lu W and Lieber C M 2004 *Nature* **420** 61
- [5] Verheijen M A, Immink G, Smet T de, Borgstrom M T and Bakkens E P A M 2006 *J. Am. Chem. Soc.* **128** 1353
- [6] Yang C, Zhong Z and Lieber C M 2005 *Science* **310** 1304
- [7] Liu T Y, Liao H C, Lin C C, Hu S H and Chen S Y 2006 *Langmuir* **22** 5804
- [8] Yang P D, Yan H Q, Mao S, Russo R, Johnson J, Saykally R, Morris N, Pham J, He R R and Choi H J 2002 *Adv. Funct. Mater.* **12** 323
- [9] Wang X D, Song J H, Summers C J, Ryou J H, Li P, Dupuis R D and Wang Z L 2006 *J. Phys. Chem. B* **110** 7720
- [10] Song J J and Lim S W 2007 *J. Phys. Chem. C* **111** 596
- [11] Ma T, Guo M, Zhang M, Zhang Y J and Wang X D 2007 *Nanotechnology* **18** 035605
- [12] Dong A, Wang F, Daulton T L and Buhro W E 2007 *Nano Lett.* **7** 1308–13
- [13] Wang C H, Wong A S W and Ho G W 2007 *Langmuir* **23** 11960–3
- [14] Law M, Greene L E, Johnson J C, Saykally R and Yang P 2005 *Nat. Mater.* **4** 15–28